Electronic Supporting Information

Slowing translocation of single-stranded DNA by using nano-cylindrical passage self-assembled by amphiphilic block copolymer

Hiroshi Yoshida [*a], Yusuke Goto [b], Rena Akahori [b], Yasuhiko Tada [a], Shohei Terada [a], Motonori Komura [c,d], and Tomokazu Iyoda [c]

[a] Center for Technology Innovation - Materials, Research & Development Group, Hitachi Ltd., 7-1-1 Omika, Hitachi, Ibaraki 319-1292, Japan

[b] Center for Technology Innovation - Healthcare, Research & Development Group, Hitachi Ltd., 1-280 Higashi-Koigakubo, Kokubunji, Tokyo 185-8601, Japan

[c] Department of Electrical and Electronics Engineering, Numazu National College of Technology, Numzau, Shizuoka 10-8501, Japan

[d] Chemical Resources Laboratory, Tokyo Institute of Technology, 4259-R1-25, Suzukakedai, Midori-ku, Yokohama, Kanagawa 226-8503, Japan

1 Experimental methods

1.1 Materials

Amphiphilic diblock copolymers, PEO_{114}-*b*-$PMA(Az)_{34}$ and PEO_{40}-*b*-$PMA(Az)_{84}$ were synthesized by atom transfer radical polymerization.[S1] Both block copolymers self-assembled hexagonally arranged PEO cylindrical microdomains in PMA(Az) matrices. The (10) lattice spacing of the PEO microdomains in bulk PEO_{114}-*b*-$PMA(Az)_{34}$ and PEO_{40}-*b*-$PMA(Az)_{84}$ measured by small-angle X-ray scattering (SAXS) were 20 nm and 19 nm, which corresponded to 23 nm and 22 nm in center to center nearest neighbor spacing *s*, respectively.

Single-stranded polydeoxyadenylic acid (ss-poly(dA)) with polymerization degree of 60-mer was purchased from Nihon Gene Research Laboratory (Miyagi, Japan). The ss-poly(dA)s with polymerization degree of 3500-mer and 5300-mer were prepared by DNA synthesis in two step reaction by the procedure reported previously in the Supplemental Information of Reference S2.

1.2 Fabrication of device chips with PEO cylinders

The device chips were fabricated following a process illustrated in Figs. 3a-i ~ 3a-iii. First, thin film of PEO-*b*-PMA(Az) was spin coated on a homemade SiN membrane window (65 μm square) fabricated on the Si substrate (Figs. 3a-i and 3a-ii). The thickness of SiN membrane was 30 nm. Prior to the coating, a single through-hole with a diameter of 50 nm was fabricated in the central region of the SiN window by e-beam lithography. The PEO-*b*-PMA(Az) was spin-coated from toluene solution with the concentration of 1.0 wt%. Thickness of the PEO-*b*-PMA(Az) layer on the SiN membrane was adjusted to be ca. 35 nm by spin-speed and verified by measuring the step created by removing a portion of the film by sharp knife utilizing an atomic force microscope. Then, the device chips were thermally treated to self-assemble PEO cylinders perpendicularly in the block copolymer films. The

thermal treatment was carried out at 140 ºC or 110 ºC for 2 h for PEO_{114}-*b*-$PMA(Az)_{34}$ and PEO_{40}-*b*-$PMA(Az)_{84}$, respectively, followed by natural cooling to the room temperature under vacuum (Fig. 3a-iii).[S3,S4] Morphologies of the self-assembled films thus obtained were observed by a scanning electron microscope (SEM, S-4800, Hitachi High-Technologies, Tokyo, Japan) and by a spherical aberration corrected scanning transmission electron microscope (STEM, HD-2700, Hitachi High-Technologies, Tokyo, Japan). The PEO microdomains were selectively stained by RuO_4 for improved contrast under SEM and STEM observations.

1.3 DNA translocation measurement

Ionic current passing through the PEO cylinders was measured by mounting the device chip in a custom-built acrylic flow cell as schematically illustrated in Fig. S2. Separated by the device chip, two chambers (each with volume of 100 μL) were formed in the flow cell. The chambers were filled with buffer solution consisted of 1 M potassium chloride, 10 mM Tris-HCl, and 1 mM EDTA buffer at pH 7.5. For translocation experiment, ss-poly(dA) dissolved in a buffer solution was injected in the *trans* chamber, so the concentration of the ss-poly(dA) to become about 10 nM for 3500-mer and 5300-mer, and about 50 nM for 60-mer. Two Ag/AgCl electrodes were immersed in both solutions for electrical contact. A patch-clamp amplifier (Axopatch 200B, Axon instruments, Union City, CA) was used for applying a voltage to the *trans* chamber and for detecting the ionic current. The detected current was first low-pass filtered with a four-pole Bessel filter, with cutoff frequency of 2 kHz, digitized with NI USB-6281 18-bit DAQ AD converter (National instruments, Austin, TX) at 50 kHz, and recorded in a hard disk drive of a personal computer. All the measurements were performed at room temperature.

2 Conductance behaviors of device chips

First, we present initial ionic current (I) - bias voltage (V) characteristics of the device chips, which were measured before applying them to ss-Poly(dA) translocation experiments. Fig. S3a presents the I-V relation of the virgin device chip composed of PEO cylinders with diameter of d = 9 nm, which was measured with both chambers filled with pure buffer solution. A linear I-V characteristic was observed without showing any rectification effect, which was further confirmed by flipping the device chip over in the cell. These results probably imply that the cylinders were symmetric in physical shape as well as in their chemical properties. Fig. S3d presents the I-V relation of the virgin device chip composed with d = 2 nm PEO cylinders immersed in pure buffer solution. Unlike the device chip with d = 9 nm cylinders, the device chip with d = 2 nm cylinders showed rectification behavior in its I-V relation. While current increased linearly with increase in bias potential in the positive potential side, the negative side was almost insulating. Although detailed mechanism to account for the observed rectification behavior requires further studies, we suppose that such rectification could be induced by unknown structural difference in both interfaces caused on coating and annealing processes, and/or asymmetric PEO morphology induced during electrophoretic transportation of small ions in buffer solution, as well as target DNA molecules, in the cylinders.[S5]

Influence of ss-poly(dA) translocation on the PEO cylinders have to be carefully considered because the experiments exhibited large decrease in device conductance with translocation of ss-poly(dA) molecules. As presented in Figs S3a and S3d, intensity of the ionic current observed with the virgin chips before the translocation was in an order of a few nA when bias potential of 300 ~ 500 mV was applied. However, the ionic current increased dramatically after the introduction of ss-poly(dA), accompanying the appearance of current blockade events. For example, when ss-poly(dA) with polymerization degree of 3500-mer

was translocated through a device chip with d = 9 nm PEO cylinders, base ionic current increased from a few nA finally to about 95 nA at V = 500 mV (see Fig. 4a). Fig. S3b compares the *I-V* relation of the device before (plot (i)) and after (plot (ii)) the translocation of 3500-mer ss-poly(dA). Note the latter was measured after replacing the solutions in both *cis* and *trans* chambers with pure buffer solution. Although linear relation between I and V was maintained in the positive side, rectification effect appeared. Moreover, absolute ionic current became far large compared with that observed with the initial device. Similar behaviors were observed after the translocation of 5300-mer ss-poly(dA) thought d = 9 nm cylinders and 60-mer ss-poly(dA) thought d = 2 nm cylinders, as presented in plots (ii) of Figs. S3c and S3e.

These behaviors may imply occurrences of large conformational changes in the PEO chains composing the cylinders or, in the worst case, breakage of the PEO-*b*-PMA(Az) thin films covering the pre-fabricated holes. We believe that the latter was not the case because clear blockade events were observed even after the increase in the ionic current. If the PEO-*b*-PMA(Az) thin films were damaged forming macroscopic openings, the blockade events corresponding to the translocation of single molecules should not be observed. This speculation was further supported by the following experiment. Plot (ii) of Fig. S3e shows the *I-V* behavior of the device chip with d = 2 nm cylinders observed after replacing the solutions in both chambers by neat buffer after the translocation of 60-mer ss-poly(dA). As mentioned above, absolute ionic current became far large compared to that observed with the initial device before introducing the ss-poly(dA) (Fig. S3d and Fig. S3e, plot (i)). Next, we have recovered the device chip from the flow cell, rinsed with pure water, dried, remounted in the flow cell, and then refilled with the buffer. The *I-V* relation then measured was almost recovered to its initial behavior as shown in plot (iii) of Fig. S3e. This finding, besides with the fact that the blockade events caused by the ss-poly(dA) translocation were clearly

observed, strongly suggests that PEO cylinders were maintained even in the case when large ionic current was observed.

Although mechanism to account for the observed conductance change is under investigation and require further studies, plausible explanation can be given as follows. As PEO cylinders were assembled by PEO-*b*-PMA(Az), although one end of the PEO chains are anchored to the interface between the PEO cylinders and the surrounding PMA(Az) matrix, the other end can be locally dispersed when cylinders are wetted by aqueous solution. Therefore, introduction of DNA molecules in PEO cylinders may cause perturbation on the PEO chains and develop conformational inhomogeneity inside the cylinders. This effect may cause change in their conductance. Here it should be important to take electrostatic force exert on PEO chains under bias potential into account. PEO chains immersed in electrolyte solution are known to be positively charged, because the chains form complexes with cationic spices in the buffer solution. This was directly proved by Berzukoc et al., Robertson et al., and Rodriguess et al., who have experimentally demonstrated the translocation of PEO chains through biological nanopores by applying bias potential.[S6-S8] Therefore, PEO chains forming cylinders could be electrophoretically dragged in direction toward the anode, *i.e.* to *cis*-chamber side, during the translocation experiments. This force may disentangle PEO chains in the cylinders with large inhomogeneity.

3 Distribution of translocation events.

Capture of DNA molecules into nanopores should be a Poisson process, in which events occur continuously and independently at a constant average rate.[S9-S11] Therefore, distribution of the interval time (δt) between successive current blockade events should obey exponential distribution: $P(\delta t) = A \exp(-R_c \cdot \delta t)$, where *Rc* is the ss-Poly(dA) capture rate.[S11] Figure S4 presents semi-exponential plot of δt distributions observed for the translocation of ss-

Poly(dA) with 3500-mer and 5300-mer though PEO cylinders with d = 9 nm, and ss-Poly(dA) with 60-mer through those with d = 2 nm. Lines are the fits to mono-exponential distributions P(δt), which show all translocation events reasonably obey a Poisson process as expected. Capture rate R_c is a function of ss-Poly(dA) concentration in the *cis*-chamber, bias potential and in the current case, number of the through PEO cylinders connecting across the device chip. The R_c value extracted from the fits were 0.024 msec^{-1} for the translocation of both 3500-mer and 5300-mer ss-Poly(dA)s with initial concentration of 10 nM across the device chip composed with three PEO cylinders with d = 9 nm, and 0.076 msec^{-1} for the translation of 60-mer with 50 nM across the device chip composed with seven PEO cylinders with d = 2 nm. Although bias potential applied for the translocation is different for each experiment, we believe it is reasonable to observe lager R_c for the translocation of 60-mer with higher concentration through the device composed with larger number of PEO cylinders. Such stochastic treatment should be powerful to understand he translocation events correlated with pore structures and is our next interest which will be reported elsewhere.

References

S1 Y. Tian, K. Watanabe, X. Kong, J. Abe, T. Iyoda, *Macromolecules*, 2002, **35**, 3739-3747.

S2 R. Akahori, T. Haga, T. Hatano, I. Yanagi, T. Ohura, H. Hamamura, T. Iwasaki, T. Yokoi, T. Anazawa, *Nanotechnology*, 2014, **25**, 275501.

S3 M. Komura, A. Yoshitake, H. Komiyama, T. Iyoda, *Macromolecules*, 2015, **48**, 672-678.

S4. J. Yoon, S. Y. Jung, B. Ahn, K. Heo, S. Jin, T. Iyoda, H. Yoshida, M. Ree, *J. Phys. Chem. B*, 2008, **112**, 8486–8495.

S5 M. Ali, B. Yameen, J. Cervera, P. Ramírez, R. Neumann, W. Ensinger, W. Knoll, O. Azzaroni, *J. Am. Chem. Soc*., 2010, **132**, 8338-8348.

S6 S. M. Berzukoc, I. Vodyanoy, V. A. Parsegian, *Nature*, 1994, **370**, 279-281.

S7 J. W. F. Robertson, C. G. Rodrigues, V. M. Stanford, K. A. Rubinson, O. V. Krasilnikov, J. J. Kasianowicz, *Proc. Natl. Acad. Sci.*, 2007, **104**, 8207-8211

S8 C. G. Rodriguess, D. C. Machado, S. F. Chevtchenko, O. V. Krasilnikov, *Biophys. J.*, 2008, **95**, 5186-5192.

S9 J. Larkin, R. Henley, D. C. Bell, T. Cohen-Karni, J. K. Rosenstein, M. Wanunu, *ACS Nano.* 2013, **7**, 10121–10128.

S10 M. Wanunu, J. Sutin, B. McNally, A. Chow, A. Meller, *Biophys. J.* 2008, **95**, 4716–4725.

S11 A. Meller, D. Branton, *Electrophoresis* 2002, **23**, 2583–2591

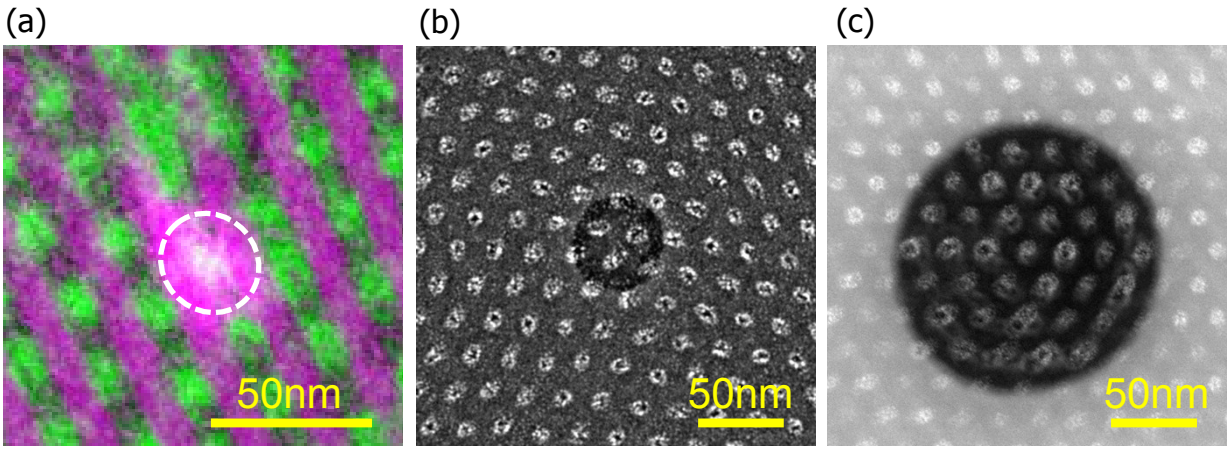

Fig. S1 Top-view electron micrographs of PEO_{114}-*b*-$PMA(Az)_{34}$ thin films self-assembled on SiN membranes each with a prefabricated hole with diameter of (a) ca. 30 nm, (b) 50 and (c) 150 nm. Image (a) was constructed by overlaying a top-view scanning electron micrograph (green) and a top-view scanning transmission electron bright-field micrograph (red) taken simultaneously by utilizing Hitachi HD-2700 microscope. Images (b) and (c) are top-view scanning transmission dark-field micrographs observed by HD-2700 microscope. Dashed line in micrograph (a) is provided to clarify the position of the underneath hole. The PEO cylinders were selectively stained by RuO_4 for improved contrast and appear bright under the dark-field transmission electron microscopy and under the scanning electron microscopy.

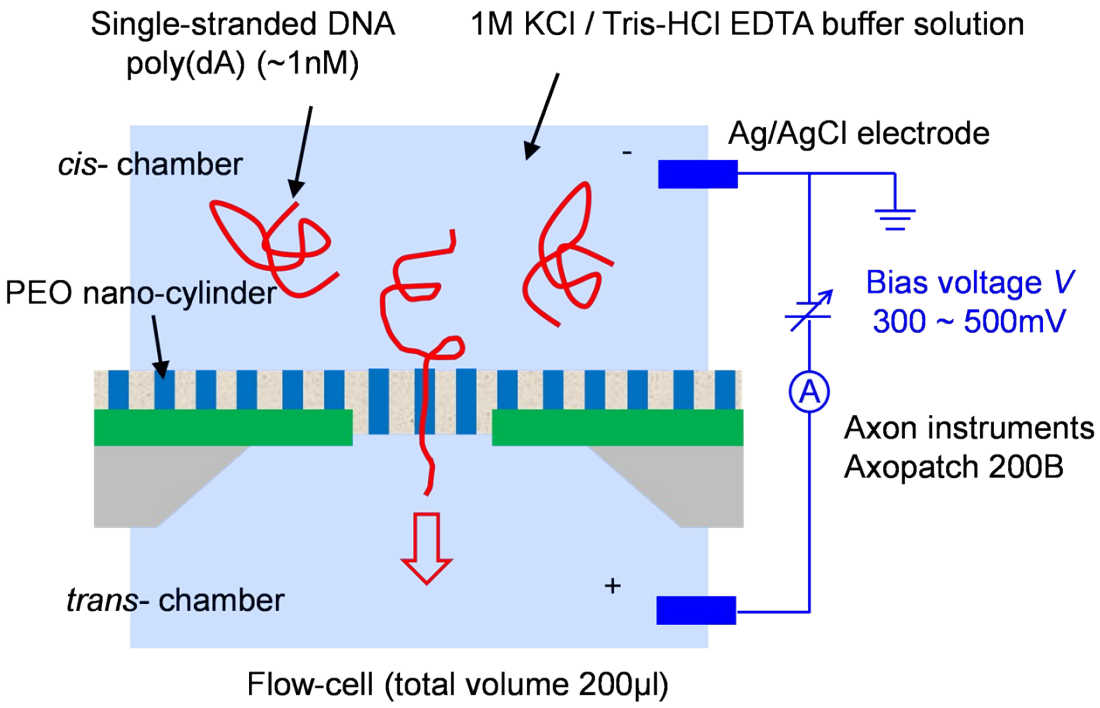

Fig. S2 Schematic illustration showing cross-section of an experimental set-up, which was utilized to measure ionic current during translocation of ssDNA molecules through PEO cylinders of a device chip.

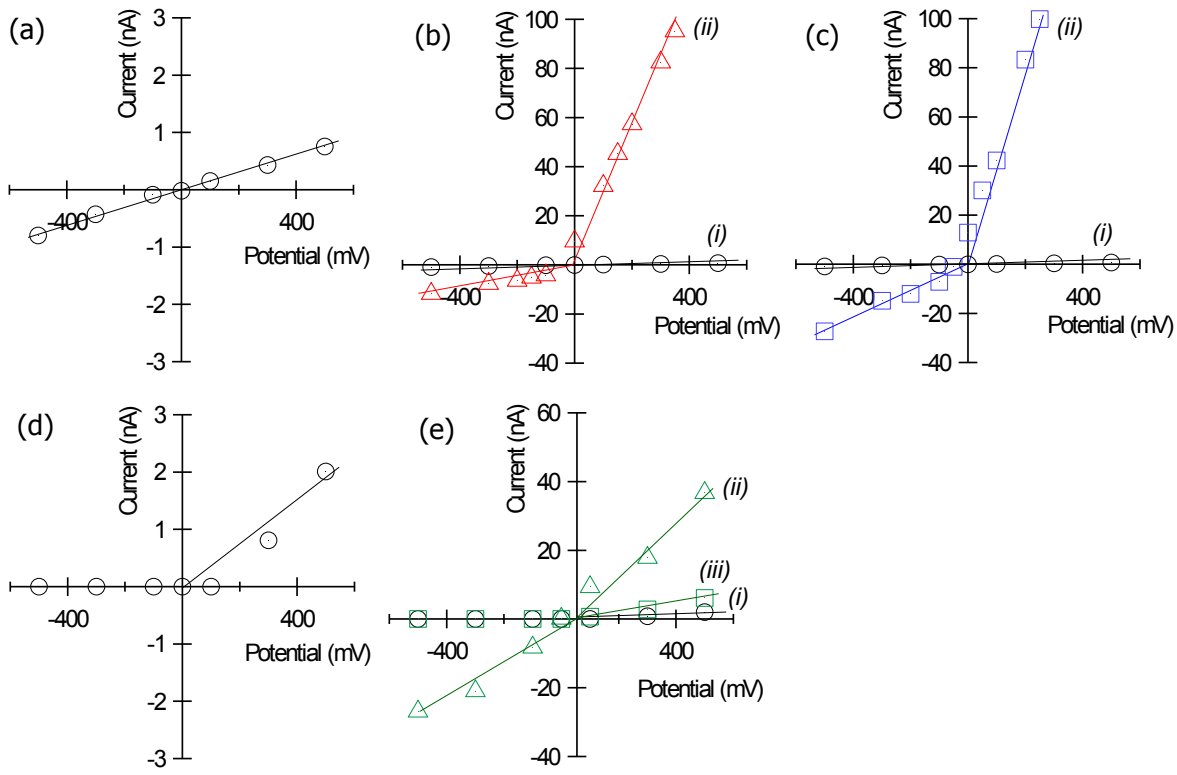

Fig. S3. Ionic current (*I*) verses bias-potential (*V*) plots measured with device chips immersed in neat buffer solution containing 1 M potassium chloride, 10 mM Tris-HCl, and 1 mM EDTA buffer at pH 7.5. (a) An *I*-*V* plot observed with a virgin device chip composed of PEO cylinders with d = 9 nm. (b)(c) *I*-*V* plots observed with device chips with d = 9 nm PEO cylinders before (plots (i)) and after (plot (ii)) the translocation of ss-poly(dA) with polymerization degrees of 3500-mer and 5300-mer, respectively. (d) *I*-*V* plot observed with a virgin device chip composed of PEO cylinders with d = 2 nm. (e) *I*-*V* plots observed with a device chip with d = 2 nm PEO cylinders before (plot (i)) after the translocation of 60-mer ss-poly(dA) (plot (ii)), and after recovering the device chip from the flow cell, rinsed with pure water, dried, remounted in the flow cell, and then refilled with the buffer (plot (iii)). Plots (ii) in (b)(c)(e) were measured by replacing the ss-Poly(dA) containing solutions in both *cis* and *trans* chambers with pure buffer solution after the translocation experiments. The device

chips with d = 9 nm and d = 2 nm PEO cylinders were fabricated with PEO_{114}-*b*-$PMA(Az)_{34}$ and PEO_{40}-*b*-$PMA(Az)_{84}$, respectively.

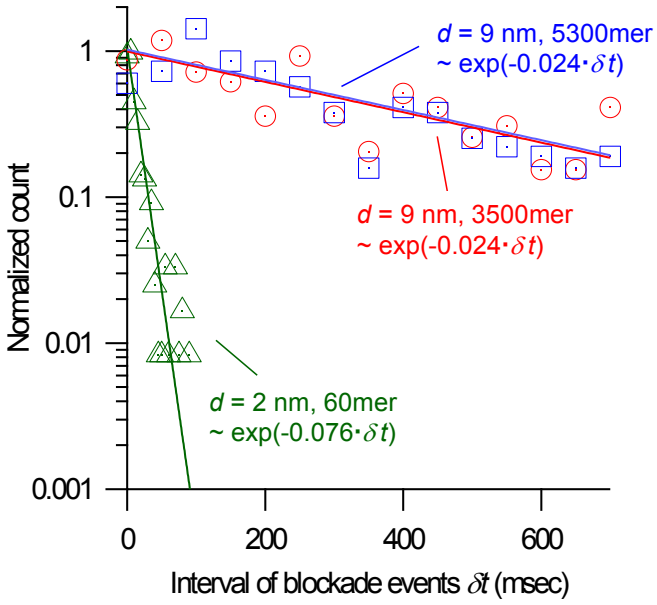

Fig. S4. Distributions of interval time (δt) between successive current blockade events observed for the translocation of ss-Poly(dA) with 3500-mer (circles in red) and 5300-mer (squares in blue) though PEO cylinders with d = 9 nm, and ss-Poly(dA) with 60-mer through those with d = 2 nm (triangles in green), driven under bias potential of V = 500 mV, 300 mV and 400 mV, respectively. Lines are fits to exponential distributions. The δt distributions were extracted from the same data-sets to construct dwell time distributions presented in Figure 5. Initial concentration of ss-poly(dA) in *cis*-chambers were ca. 10 nM for 3500-mer and 5300-mer, and ca. 50 nM for 60-mer.